Journal of Rare Earths 36 (2018) 281–286

Contents lists available at ScienceDirect

Journal of Rare Earths

journal homepage: http://www.journals.elsevier.com/journal-of-rare-earths

Effect of niobium substitution on microstructures and thermal stability of $TbCu_7$-type Sm–Fe–N magnets☆

Guiyong Wu [a], Hongwei Li [a, *], Dunbo Yu [a], Kuoshe Li [a], Wenlong Yan [a], Chao Yuan [a], Liang Sun [a], Yang Luo [a], Kun Zhang [a, b, **]

[a] National Engineering Research Center for Rare Earth Materials, General Research Institute for Nonferrous Metals, Grirem Advanced Materials Co. Ltd., Beijing 100088, China

[b] Key Laboratory of Microgravity (National Microgravity Laboratory), Institute of Mechanics, Chinese Academy of Sciences, Beijing 100190, China

ARTICLE INFO

Article history:
Received 13 February 2017
Received in revised form
2 May 2017
Accepted 3 May 2017
Available online 18 August 2017

Keywords:
Magnetic properties
Thermal stability
Grain size
Pinning field
Irreversible flux loss
Rare earths

ABSTRACT

This paper reports crystal structures, magnetic properties and thermal stability of $TbCu_7$-type $Sm_{8.5}Fe_{(85.8-x)}Co_{4.5}Zr_{1.2}Nb_x$ ($x = 0$–1.8) melt-spun compounds and their nitrides, investigated by means of X-ray diffraction, vibrating sample magnetometer, flux meter and transmission electron microscope. It is found that the lattice parameter ratio c/a of $TbCu_7$-type crystal structure increases with Nb substitution, which indicates that the Nb can increase the stability of the metastable phase in the Sm–Fe ribbons. Nb substitution impedes the formation of magnetic soft phase α-Fe in which reversed domains initially form during the magnetization reversal process. Meanwhile, Nb substitution refines grains and leads to homogeneous microstructure with augmented grain boundaries. Thus the exchange coupling pining field is enhanced and irreversible domain wall propagation gets suppressed. As a result, the magnetic properties are improved and the irreversible flux loss of magnets is notably decreased. A maximum value 771.7 kA/m of the intrinsic coercivity H_{cj} is achieved in the 1.2 at% substituted samples. The irreversible flux loss for 2 h exposure at 120 °C declines from 8.26% for Nb-free magnets to 6.32% for magnets with 1.2 at% Nb substitution.

1. Introduction

Initially discovered by Katter et al in 1991,[1] the stoichiometric $SmFe_9N_x$ intermetallic compounds in the hexagonal $TbCu_7$-type structure have excellent intrinsic magnetic properties with high Curie temperature (743 K),[1] high saturation magnetization (1.70 T)[2] and large anisotropy fields. Combined with good resistance to oxidation, the $TbCu_7$-type Sm–Fe–N material has been considered to be one of the promising permanent magnetic materials in the field of small instruments such as miniature motors, actuators, and sensors.[3]

Since the discovery of $TbCu_7$-type Sm–Fe–N compounds, material researchers have already made some achievements in enhancing the magnetic properties, either by the improvement of preparation technology or the substitution of new elements.[4–6] Previous studies indicate that Zr or Hf addition can stabilize the $TbCu_7$-type metastable phase and Co addition is able to enhance the Curie temperature of Sm $(Fe,Co)_7$ compound. Meanwhile, high performance $TbCu_7$-type nanocrystalline Sm–Fe–N compounds with additions of Zr, Co, Nb, B elements had been prepared by many researchers.[7–9] However, one of the major drawbacks of $TbCu_7$-type Sm–Fe–N bonded magnets is the poor thermal stability, which limits their application at high temperature. Lately researches on MnBi/SmFeN hybrid bonded magnets show that high coercivity MnBi improves the thermal stability of hybrid magnets.[10] Also more works are concentrating on the $Sm_2Fe_{17}N_x$ type magnetic material with pure phase and fine grain structure.[11,12] Unfortunately, seldom researchers have studied the thermal stability and magnetization reversal behavior of isotropic $TbCu_7$-type Sm–Fe–N magnets.

☆ **Foundation item:** Project supported by the National Natural Science Foundation of China (51401028).

* Corresponding author. National Engineering Research Center for Rare Earth Materials, General Research Institute for Nonferrous Metals, Grirem Advanced Materials Co. Ltd., Beijing 100088, China.

** Corresponding author. Key Laboratory of Microgravity (National Microgravity Laboratory), Institute of Mechanics, Chinese Academy of Science, Beijing 100190, China.

E-mail addresses: lihw0923@126.com (H.W. Li), zhangkun@imech.ac.cn (K. Zhang).

http://dx.doi.org/10.1016/j.jre.2017.05.008
1002-0721/

Recent studies on melt-spun Nd–Fe–B nanocrystalline magnets show that Nb substitution refines the grain structure and enhances the exchange coupling pinning field.[13] Nb also increases the nucleation field for irreversible magnetization reversal in $TbCu_7$-type SmCo-based magnets.[14] Then will Nb substitution have similar effects in $TbCu_7$-type Sm–Fe–N magnets? The present work focuses on the role of Nb substitution in the Sm–Zr–Fe–Co system alloy, which may shed some lights on enhancing the magnetic properties of $TbCu_7$-type Sm–Fe–N bonded magnets.

2. Experimental

The compounds of nominal composition of $Sm_{8.5}Fe_{(85.8-x)}Co_{4.5}Zr_{1.2}Nb_x$ (x = 0, 0.3, 0.6, 0.9, 1.2, 1.5, 1.8) were prepared by melt spinning method under 50 m/s surface velocity in Ar atmosphere. The precursors were melted from Sm, Fe, Co, Zr, and NbFe (purity 99.9%) constituent elements under argon using an induction melting furnace. The as-quenched ribbons were annealed at temperature of 800 °C for 1 h in an Ar-flowing tube furnace. Then Sm–Fe–Co–Zr–Nb powders pulverized and sieved under 110 μm were nitrided at 450 °C for 24 h in nitrogen atmosphere. Magnetic properties of nitrides were measured at room temperature using a vibrating sample magnetometer (VSM, Quantum Design Versalab) with a maximum applied field of 3 T. X-ray diffraction (XRD) analysis was carried out with a Rigaku Smartlab Diffractometer using Co Kα radiation. The microstructure of ribbons was characterized with a transmission electron microscope (TEM, FEI TECNAI F20). Bonded magnets were prepared by mixing magnetic powders and epoxy resin in the proportion of 100:4. The mixture was pressed into cylinders with the size of ∅ 10 mm × 7 mm (Permeance coefficient, P_c = 2) and the density of 5.85 g/cm^3. The bonded magnets were cured at 175 °C for 1.5 h. And then, the bonded magnets were magnetized in a pulse magnetic field of 4 T. Finally, the demagnetization curves of bonded magnets were measured using NIM-500C hysteresis graph instrument. Both the initial flux and the irreversible flux loss after heat treatment were measured with a flux meter at room temperature.

3. Results and discussions

3.1. Phase evolution and structure

Fig. 1(a) shows the XRD diffraction patterns of as-quenched $Sm_{8.5}Fe_{(bal-x)}Co_{4.5}Zr_{1.2}Nb_x$ ribbons. The $TbCu_7$-type metastable phase is dominant in the as-quenched ribbons. As shown in Fig. 1, a small amount of Nb substitution can suppress the precipitation of $Sm_2(Fe,M)_{17}$ phase. With the Nb content increasing, the diffraction peaks of $TbCu_7$ structure become broadened and scattered, which implies that Nb substitution stabilizes the residual amorphous phase.[15] Fig. 1(b) gives the XRD patterns of as-annealed (at 800 °C) Sm–Fe ribbons. The strengthened characteristic diffraction peaks indicate better crystallization in the ribbons. The phase structure of Nb-free sample is composed of soft magnetic phase α-Fe and Sm-rich phase, however, the specimens with Nb substitution contain scarce α-Fe and no Sm-rich phase. Furthermore, the mean grain size of as-annealed ribbons notably decreases with Nb substitution, from about 60 nm at x = 0 to about 30 nm at x = 1.2, according to Scherrer equation. Fig. 1(c) illustrates the variation of lattice parameters and axial ratio c/a value versus the content of Nb element. With the increase of Nb content, the lattice parameter a decreases and the c increases, as a result, a noticeable expansion of c/a value is observed. In fact, the greater the ratio of c/a, the more the stable $TbCu_7$-type crystal structure.[16] The results in Fig. 1(c) manifest that Nb substitution also promotes the stability of $TbCu_7$-type metastable phase in the Sm–Fe ribbons. Fig. 1(d) shows the XRD patterns of Sm–Fe–Co–Zr–Nb nitrides. Fig. 1(d) indicates that the diffraction peaks have an obvious left-shift after nitriding, which shows N atoms have penetrated into the crystal structure.[17]

3.2. Improvement of magnetic properties

The room temperature magnetic properties, remanence B_r, coercivity H_{cj} and energy product $(BH)_{max}$ of $Sm_{8.5}Fe_{(85.8-x)}Co_{4.5}Zr_{1.2}Nb_x$ (x = 0–1.8) nitrides are listed in Table 1. With a small amount of Nb substitution (x = 0.3, 0.6), the coercivity slightly increases, but the remanence decreases remarkably. This is mainly because that the microstructure of the ribbons is hardly modified with a little Nb content, and saturation magnetization is reduced as Nb atoms substitute some Fe atoms. As Nb substitution increases from x = 0.6 to x = 1.2, the grain structures are refined and the intergranular exchange gets enhanced, the coercivity of the Sm–Fe–N increases gradually. The sample with 1.2 at% Nb reaches the maximum coercivity 771.7 kA/m. It should be noted that magnetic properties of Sm–Fe–N have an obvious deterioration with over 1.5 at% Nb substitution. Because overfull Nb substitution (x > 1.5) stabilizes the residual amorphous that hinders the interaction between grains. Overfull Nb substitution also gives birth to more α-Fe phase. The soft magnetic phase exists among grains which can weaken the intergranular interaction, thus the magnetic properties of the samples decrease.[18–20] The optimum magnetic properties of $TbCu_7$-type Sm–Fe–N are achieved: B_r = 827.3 mT, H_{cj} = 771.7 kA/m, and $(BH)_{max}$ = 90.1 kJ/m^3.

Fig. 2 depicts the hysteresis loops of optimum Nb substitution (x = 1.2) sample and Nb-free sample, and the inset indicates the XRD diffraction patterns of their powders. Nb substitution reduces the soft magnetic phase α-Fe in the nitride and smoothes the demagnetization curve graphically.

3.3. Thermal stability improvement of bonded magnets

To have a further understanding of the effect of Nb substitution on thermal stability, the two types of $Sm_{8.5}Fe_{85.8}Co_{4.5}Zr_{1.2}N_\delta$ and $Sm_{8.5}Fe_{84.6}Co_{4.5}Zr_{1.2}Nb_{1.2}N_\delta$ bonded magnets (named as NB0 and NB12 magnets for convenience) were prepared to investigate the thermal demagnetization curve and irreversible flux loss. The magnetic properties of materials are listed in Table 2.

The thermal stability of permanent magnetic materials is usually manifested by thermal demagnetization curves and irreversible flux loss (h_{irr}). The demagnetization curves of bonded magnets were measured directly with NIM-500C hysteresis graph instrument. The irreversible flux loss, h_{irr}, average temperature coefficients $\overline{\alpha}$ and $\overline{\beta}$ were calculated from[21]:

$$h_{irr} = \frac{\phi'(T_0) - \phi(T_0)}{\phi(T_0)} \times 100\% \quad (1)$$

$$\overline{\alpha} = \frac{h_{irr}}{(T_{ex} - T_0)} \quad (2)$$

$$\overline{\beta} = \frac{H(T_{ex}) - H(T_0)}{H(T_0)(T_{ex} - T_0)} \times 100\% \quad (3)$$

Here $\phi(T_0)$ and $\phi'(T_0)$ are the flux value measured at room temperature before and after the exposure at T_{ex}. $H(T_{ex})$ and $H(T_0)$ are the coercivity measured at exposure temperature T_{ex} and room temperature T_0. The open-circuit flux of magnets due to an exposure at certain temperature, T_{ex}, was measured by the sample-extraction method.

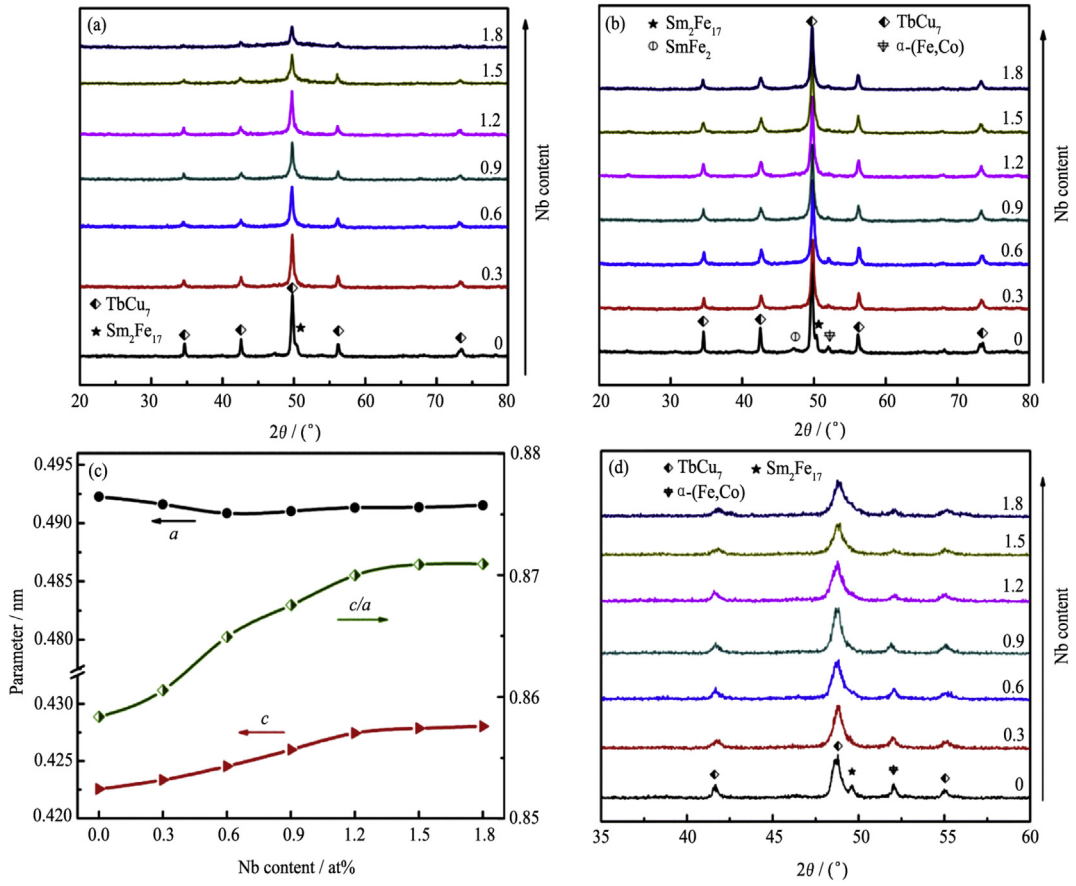

Fig. 1. XRD patterns of as-quenched (a), as-annealed (b) $Sm_{8.5}Fe_{(85.8-x)}Co_{4.5}Zr_{1.2}Nb_x$ ribbons ($v = 50$ m/s) and its nitrides (d), the dependence of the unit cell parameters a, c and the axial ratio c/a on the Nb content (c).

Table 1
Dependence of magnetic properties on Nb content for $Sm_{8.5}Fe_{(85.8-x)}Co_{4.5}Zr_{1.2}Nb_x$ nitrides.

Nb content (at%)	B_r (mT)	H_{cj} (kA/m)	$(BH)_{max}$ (kJ/m^3)
$x = 0$	835.5	629.6	92.1
$x = 0.3$	781.8	626.8	73.4
$x = 0.6$	799.3	639.2	78.0
$x = 0.9$	794.7	724.3	80.3
$x = 1.2$	827.3	771.7	90.1
$x = 1.5$	787.8	733.1	72.1
$x = 1.8$	716.5	640.1	68.8

As seen in Fig. 3, the demagnetization curves of Sm–Fe–N bonded magnets appear to become compact at high temperature, reflecting obvious deterioration of magnetic properties. However, the remanence B_r of NB12 magnets shows less decay at high temperature (150 °C): 8.61% total loss for NB12 magnets versus 10.1% loss for NB0 magnets. The results indicate that magnets with Nb substitution have a better performance in maintaining the magnetization than magnets without Nb.

Fig. 4 illustrates the dependence of irreversible flux loss on exposure temperature (60 °C, 90 °C, 120 °C, 150 °C, 170 °C) and corresponding remanence temperature coefficient $\overline{\alpha}$. For any given exposure temperature, the irreversible flux loss of NB12 magnets is always about 2% less than that of NB0 magnets. Also, the remanence temperature coefficient $\overline{\alpha}$ (the dotted line) of NB12 magnets decreases notably. Fig. 5 presents the long-term irreversible flux loss of magnets exposed at 120 °C as a function of exposure time.

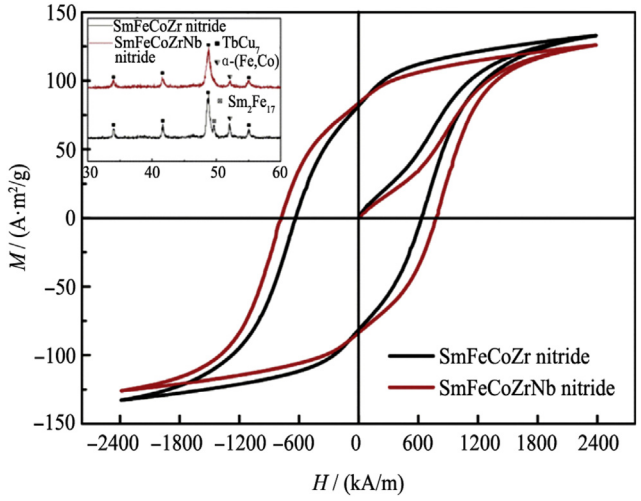

Fig. 2. Hysteresis loops of $Sm_{8.5}Fe_{85.8}Co_{4.5}Zr_{1.2}$ nitride and $Sm_{8.5}Fe_{84.6}Co_{4.5}Zr_{1.2}Nb_{1.2}$ nitride. The inset shows XRD patterns of their nitride powders.

The initial flux loss of NB12 magnets is approximately 2% lower than NB0 magnets. More importantly, the long-term (500 h) flux loss of NB12 magnets slumps to 11.5%, in comparison with 14.7% of NB0 magnets. It is confirmed that Nb substitution improves the thermal stability of $TbCu_7$-type Sm–Fe–N and reduces the irreversible flux loss of bonded magnets.

Table 2
The magnetic properties of $TbCu_7$-type Sm–Fe–N compounds and its bonded magnets.

Nb content		B_r (mT)	H_{cj} (kA/m)	$(BH)_{max}$ (kJ/m^3)	$\overline{\alpha}$ (%/°C)	$\overline{\beta}$ (%/°C)
Nb = 0	Powder	844.9	651.5	92.1		
	Magnet	660.9	646.1	64.6	−0.080	−0.376
Nb = 1.2	Powder	843.7	737.3	91.5		
	Magnet	683.7	729.1	68.3	−0.062	−0.399

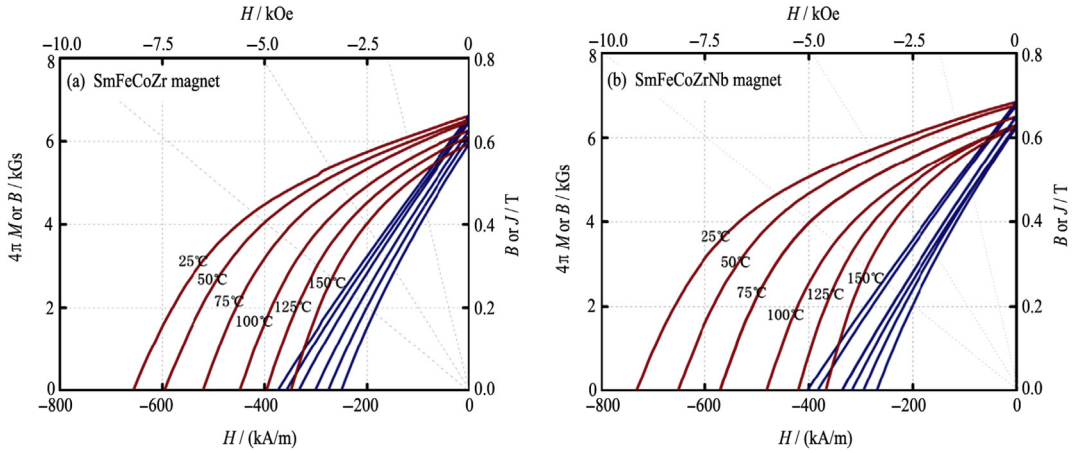

Fig. 3. Thermal demagnetization curves of NB0 magnets (a) and NB12 magnets (b).

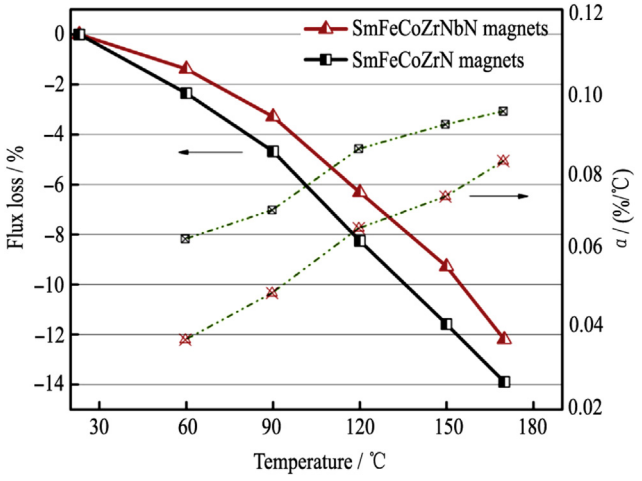

Fig. 4. Irreversible flux loss of bonded magnets due to 2-h exposure at elevated temperature and calculated remanence temperature coefficient $\overline{\alpha}$.

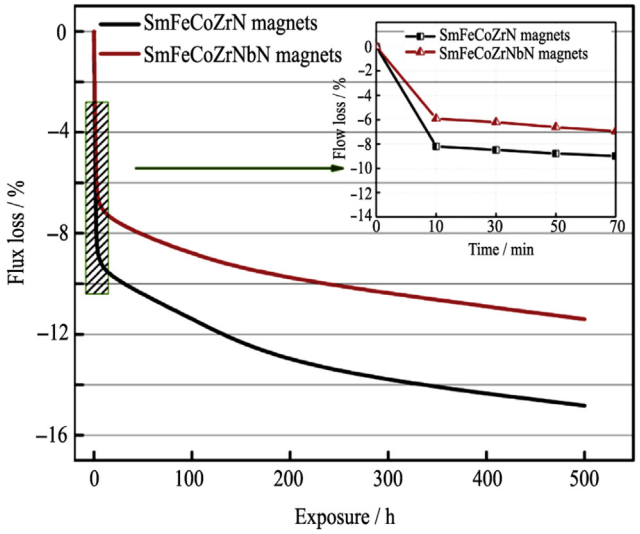

Fig. 5. Long-term irreversible flux loss of bonded magnets as a function of exposure time (120 °C in the air). The inset is the replay of initial (1 h) flux loss.

3.4. Microstructure improvement

There is a strong connection between microstructure and magnetic properties in $TbCu_7$-type Sm–Fe–N materials. Since the thermal stability can be improved with Nb substitution, it is indispensable to unveil the details of microstructure evolution and its effects on the thermal stability.

The microstructure of $Sm_{8.5}Fe_{85.8}Co_{4.5}Zr_{1.2}$ and $Sm_{8.5}Fe_{84.6}Co_{4.5}Zr_{1.2}Nb_{1.2}$ ribbons (named as NB0 and NB12 ribbons) after annealing at 800 °C for 1 h is shown in Fig. 6. The inset shows the selected area diffraction patterns (SAED). As for NB0 ribbons, the microstructure is rather inhomogeneous, and the grain size ranges from 50 to 100 nm (see bar chart in Fig. 6(a)). The SAED patterns confirm the $TbCu_7$-type metastable phase and α-Fe phase in NB0 ribbons. In comparison, the microstructure of NB12 ribbons becomes much homogeneous as shown in Fig. 6(b). The grain structure has a relative small size distribution and the averaged grain size is 35 nm. Besides, polycrystalline diffraction rings in the SAED patterns indicate scarce α-Fe phase in NB12 ribbons. Small grains and uniform grain boundary are favored by exchange coupling interaction.[22,23] The result of TEM micrograph demonstrates Nb substitution effectively refines the grain structure. Therefore the magnetic properties of the alloy are notably enhanced.

Fig. 7 shows HRTEM micrographs of NB0 and NB12 ribbons. The grain structure of NB0 ribbons comprises $TbCu_7$-type grains and α-Fe grains with bar or cuneiform shape. The inhomogeneous and

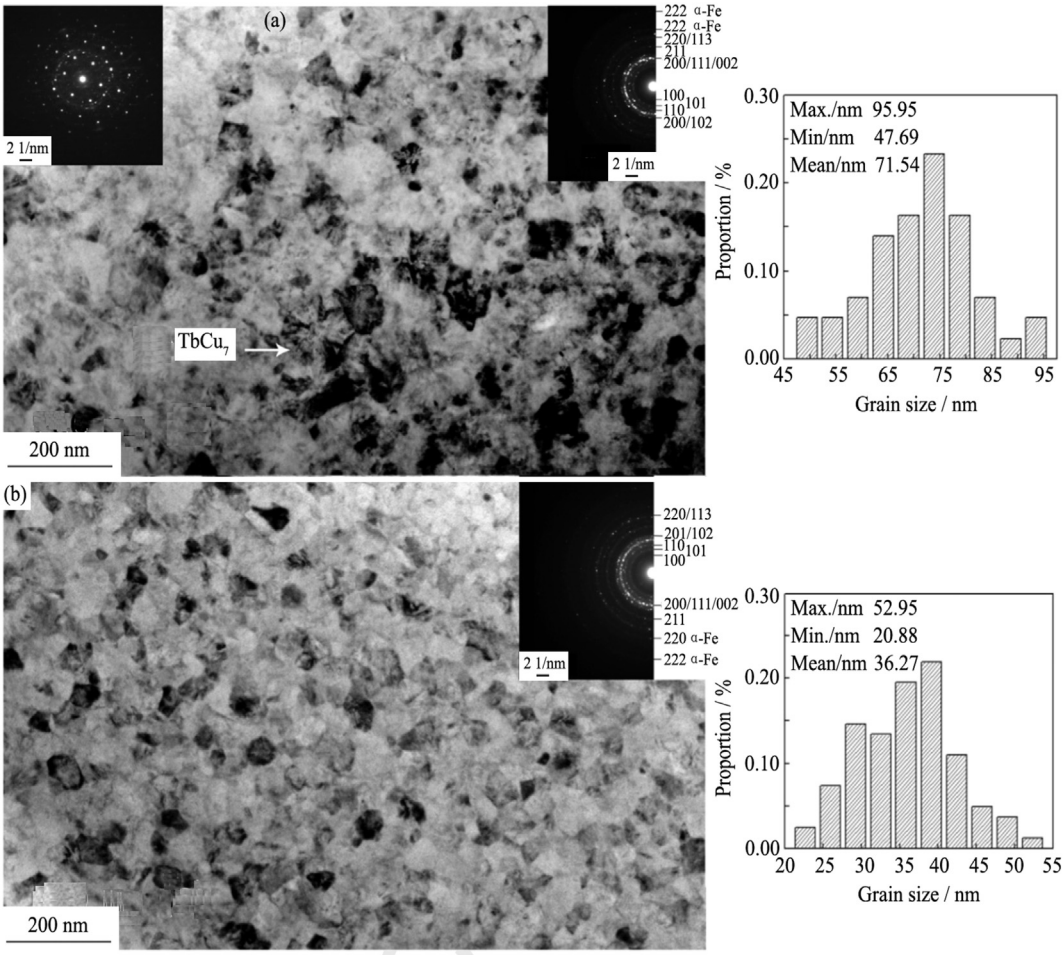

Fig. 6. TEM micrographs and SAED patterns (inset) of as-annealed NB0 ribbons (a) and NB12 ribbons (b).

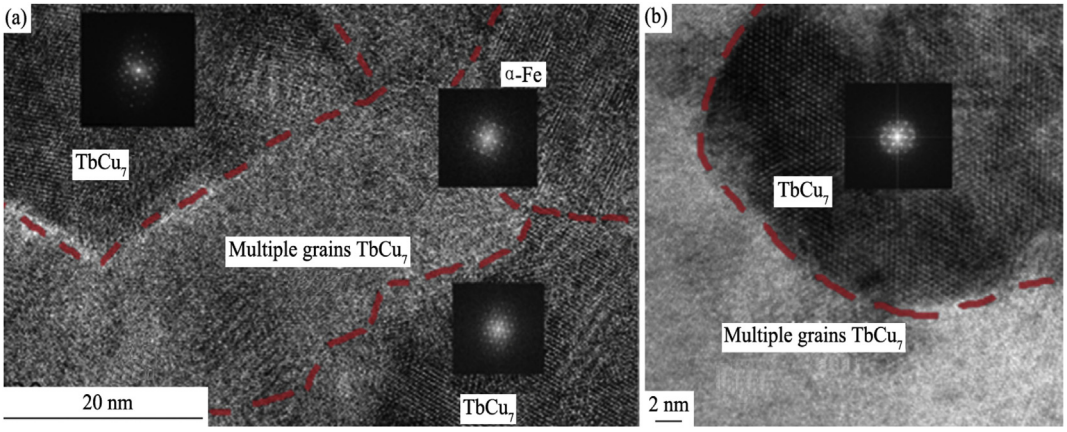

Fig. 7. The HRTEM micrograph of as-annealed NB0 ribbons (a) and NB12 ribbons (b).

irregular grains cause high inner dispersal magnetic field, which increases the magnetic domain reversal. On the contrary, the grain boundary of NB12 ribbons is much smooth, suggesting small inner dispersal magnetic field. The better microstructure is the main reason of the magnetic properties enhancement in the Nb-substituted alloy.

The microstructure is a crucial factor that affects the thermal stability of Sm–Fe–N magnets. In nanocomposite magnets, the process of magnetization reversal mainly includes domain nucleation, pinning effect on domain wall motion and exchange coupling between grains.[24] The nucleation of reversed domain occurs in those districts with low effective anisotropy field in magnetic materials. And the domain wall will propagate by passing through grain boundary. However, it is the exchange coupling pinning effect that predominantly suppresses the movement of irreversible domain wall into neighbor grains with high effective anisotropy.[22–26] The exchange coupling pinning field can be calculated from the formula as follows:

$$H_p = \frac{2K_1^H}{\mu_0 M_s} \times \frac{\delta_B^H}{\pi r_0} - N_{eff} M_s \quad (4)$$

Here K_1^H is the magneto-crystalline anisotropic constant of hard phase and r_0 is the grain size of soft phase. It is obvious that the exchange coupling pining field is in proportion to anisotropic field $H_A^K = 2K_1^H/\mu_0 M_s$ and in inverse proportion to the soft grain size.

Nb substitution notably refines the grain structure and increases the fraction of grain boundary. As a result, the exchange coupling pinning field is increased, and the irreversible domain movement is suppressed under thermal fluctuation. Besides, Nb substitution impedes the formation of α-Fe grains. Since the nucleation of reversed domain forms in such regions with low effective anisotropy,[27] the initial reversed domain volume can be reduced. More importantly, the homogeneous grain structure with less irregular or cuneiform grains leads to lower inner dispersal magnetic field, which reduces the magnetization reversal and helps maintain the flux.[28] Consequently, the irreversible flux loss of magnets with Nb substitution is significantly decreased and the thermal stability gets improved.

4. Conclusions

A certain amount of Nb substitution significantly enhances the coercivity of Sm–Fe–N compounds. With 1.2 at% Nb substitution, the optimum magnetic properties of $TbCu_7$-type Sm–Fe–N are achieved: $B_r = 827.3$ mT, $H_{cj} = 771.7$ kA/m, and $(BH)_{max} = 90.1$ kJ/m^3. Nb substitution considerably reduces the irreversible flux loss of Sm–Fe–N bonded magnets as well as the remanence temperature coefficient $\bar{\alpha}$. For NB12 magnets, the 2-h irreversible flux loss at 120 °C is 6.32% and $\bar{\alpha}$ is −0.065%/°C.

Nb substitution leads to homogeneous microstructure with small and regular grains in the alloy, therefore the exchange coupling pinning field gets enhanced and the inner dispersal magnetic field is suppressed. Meanwhile, Nb substitution also impedes the formation of α-Fe soft magnetic phase, resulting in the decrease of nucleation of reversed domain. As a result, the irreversible flux loss is decreased and the thermal stability is improved in the $TbCu_7$-type Sm–Fe–N magnets.

Acknowledgment

The authors would like to thank Zhiwei Du and her co-workers for performing the transmission electron microscopy experiments and thank Zilong Wang for guiding the analysis of the selected area diffraction patterns.

References

1. Katter M, Wecker J, Schultz L. Structural and hard magnetic properties of rapidly solidified Sm–Fe–N. *J Appl Phys*. 1991;70(6):3188.
2. Sakurada S, Hirai T, Tsutai A. Potential of iron-rich R–Zr–Fe alloys for use in permanent magnets. *J Magn Soc Jpn*. 1997;21:181.
3. Omatsuzawa R, Murashige K, Iriyama T. Magnetic properties of $TbCu_7$-type Sm–Fe–N melt-spun ribbons. *Trans Magn Soc Jpn*. 2004;4(4):113.
4. Omatsuzawa R, Murashige K, Iriyama T. Structure and magnetic properties of SmFeN prepared by rapid-quenching method. *Magn Mater Semicond Jpn*. 2002;73(4):235.
5. Yamamoto H, Mori T. Magnetic properties of $TbCu_7$-type Sm–Fe–Co–Ti–N compounds. *J Jpn Soc Powder Powder Metall*. 2003;50(11):865.
6. Quan NT, Zhang SR, Yu DB, Li KS, Luo Y, Jin JY, et al. Crystal structure and hard magnetic properties of $TbCu_7$-type $Sm_{0.98}Fe_{9.02-x}Ga_x$ nitrides. *J Rare Earths*. 2014;32(8):722.
7. Sakurada S, Tsutai A, Hirai T, Yanagida Y, Sahashi M. Structural and magnetic properties of rapidly quenched (R, Zr)(Fe, Co)$_{10}N_x$ (R=Nd, Sm). *J Appl Phys*. 1996;79(8):4611.
8. Mochizuki M, Shimizu M, Murakawa M, Tanigawa S. Magnetic properties and crystal structures of nanocrystalline Sm–Fe–Co–Nb–B compounds. *J Jpn Soc Powder Powder Metall*. 2003;50(1):22.
9. Yamamoto H, Matsumoto S, Fukuno A. Magnetic properties of $TbCu_7$-type Sm–Fe–Co–Nb–Zr system nitriding compounds. *J Jpn Soc Powder Powder Metall*. 2001;48(2):184.
10. Zhang DT, Geng WT, Yue M, Liu WQ, Lu QM, Zhang JX, et al. Magnetic properties and thermal stability of MnBi/SmFeN hybrid bonded magnets. *J Appl Phys*. 2014;115(17):17A746.
11. Saito T, Nishio D. Magnetic properties of Sm–Fe–N bulk magnets prepared from $Sm_2Fe_{17}N_3$ melt-spun ribbons. *J Appl Phys*. 2015;117(17):17D130.
12. Okada S, Takagi K, Ozaki K. Direct preparation of submicron-sized Sm_2Fe_{17} ultra-fine powders by reduction-diffusion technique. *J Alloys Compd*. 2016;663(1):872.
13. Zhang R, Liu Y, Ye JW, Yang WF, Ma YL, Gao SJ. Effect of Nb substitution on the temperature characteristics and microstructures of rapid-quenched NdFeB alloy. *J Alloys Compd*. 2007;427(1):78.
14. Hu CY, Pan MX, Wu Q, Ge HL, Wang XM, Lu CY, et al. Effect of niobium addition on magnetization reversal behavior for SmCo-based magnets with $TbCu_7$-type structure. *J Rare Earths*. 2016;34(1):61.
15. Wu YQ, Ping DH, Hono K, Hamano M, Inoue A. Microstructural characterization of an α-Fe/$Nd_2Fe_{14}B$ nanocomposite magnet with a remaining amorphous phase. *J Appl Phys*. 2000;87(12):8658.
16. Luo Y, Zhang K, Li KS, Yu DB, Jin JL, Men K, et al. Structure and magnetic behaviors of melt-spun SmFeSiB ribbons and their nitrides. *J Magn Magn Mater*. 2016;405(1):214.
17. Sun JB, Cui CX, Zhang Y, Li L, Gao JX, Liu YL. Structural and magnetic properties of $Sm_2Fe_{17-x}Nb_x$ (x=0~4) alloys prepared by HDDR processes and their nitrides. *Rare Met*. 2006;25(2):129.
18. Yamasaki M, Hamano M, Mizuguchi H, Kobayashi T, Hono K, Yamamoto H, et al. Microstructure of hard magnetic bcc-Fe/NdFeB nanocomposite alloys. *Scr Mater*. 2001;44(8):1375.
19. Men K, Li KS, Luo Y, Yu DB, Zhang K, Jin JL, et al. The crystallization behavior of as-quenched $Nd_9Fe_{85}Nb_{0.5}B_{5.5}$ alloys. *J Alloys Compd*. 2015;635(1):61.
20. Chen Z, Wu YQ, Kramer MJ, Smith BR, Ma BM, Huang MQ. A study on the role of Nb in melt-spun nanocrystalline Nd–Fe–B magnets. *J Magn Magn Mater*. 2004;268(1):105.
21. Zhou SZ, Dong QF. *Super Permanent Magnets-Permanent Magnetic Material of Rare-Earth and Iron System*. Beijing: Metallurgy Industry Publishing; 2004:70.
22. Schrefl T, Fidler J, Kronmüller H. Remanence and coercivity in isotropic nanocrystalline permanent magnets. *Phys Rev B*. 1994;49(9):6100.
23. Han GB, Su H, Gao RW, Yu SY, Kang SS, Zhu MG, et al. Magnetic reversal and magnetic memory effect in melt-spun $Pr_2Fe_{14}B$/α-Fe nanocomposite ribbons. *J Rare Earths*. 2015;33(12):1303.
24. Li ZB, Shen BG, Niu E, Sun JR. Nucleation of reversed domain and pinning effect on domain wall motion in nanocomposite magnets. *Appl Phys Lett*. 2013;103(6):062405.
25. Yue M, Li YQ, Liu RM, Liu WQ, Guo ZH, Li W. Abnormal size-dependent coercivity in ternary Sm–Fe–N nanoparticles. *J Alloys Compd*. 2015;637(1):297.
26. Zhang H, Rong CB, Du XB, Zhang J, Zhang SY, Shen BG. Investigation on intergrain exchange coupling of nanocrystalline permanent magnets by Henkel plot. *Appl Phys Lett*. 2003;82(23):4098.
27. Li ZB, Zhang M, Wang LC, Shen BG, Zhang XF, Li YF, et al. Investigation on intergranular exchange coupling effect in $Pr_9Fe_{85.5}B_{5.5}$ ribbons. *Appl Phys Lett*. 2014;104(5):052406.
28. Kou XC. Coercivity of SmFeN permanent magnets produced by various techniques. *J Alloys Compd*. 1998;281(1):41.